Author's Accepted Manuscript

www.elsevier.com/locate/jtherbio

Contribution of wetted clothing to body energy exchange and heat stress

John Elson, Steve Eckels

PII: S0306-4565(17)30496-5
DOI: https://doi.org/10.1016/j.jtherbio.2018.09.014
Reference: TB2183

To appear in: *Journal of Thermal Biology*

Received date: 19 December 2017
Revised date: 19 September 2018
Accepted date: 19 September 2018

Cite this article as: John Elson and Steve Eckels, Contribution of wetted clothing to body energy exchange and heat stress, *Journal of Thermal Biology,* https://doi.org/10.1016/j.jtherbio.2018.09.014

Contribution of wetted clothing to body energy exchange and heat stress

John Elson*, Steve Eckels
Department of Mechanical and Nuclear Engineering, Institute for Environmental Research, Kansas State University, 64 Seaton Hall, Manhattan, KS, 66506, USA

***Corresponding Author** John Elson Ford Motor Company jcelson@ksu.edu

Abstract
Quantifying the impact of clothing thermal and evaporation resistance is essential to providing representative boundary conditions for physiological modeling. In many models, sweat is assumed to drip off the skin surface to the environment and is not captured in clothing. In high metabolic rate and high temperature and humidity conditions the sweat produced by the body has the potential to saturate semipermeable clothing ensembles, changing the assumptions of the model. Workers, athletes and soldiers commonly wear encapsulating versions of such clothing to protect against environmental hazards. A saturated clothing model is proposed based on the ASHRAE two-node model using a saturated spot element in parallel with the existing method to account for sweat absorbed in the clothing. The work uses fundamental heat and mass transfer principles, modifying the existing formula using clothing measurements and basic assumptions. The effectiveness of the model is demonstrated by comparing the predictions of the original and proposed models, to the results of 21 soldiers exercising. The soldiers wore combat pants and shirt, helmet, gloves, shoes, socks, and underwear, and walked in a thermal chamber for 2 h at 42.2 °C dry bulb temperature, 54.4 °C wet bulb temperature, 20% relative humidity, and airspeed of 2 m/s. Core temperature, seven skin temperatures, heart rate, and total sweat loss were measured. The original model provides an average core temperature difference compared with the human subject results of 1.31 °C (SD=0.557 °C) while the modified model improves the final prediction of core temperature to within an average of 0.15 °C (SD=0.383 °C). The new model shows an improvement in the prediction of human core temperature under the tested conditions where dripping sweat will saturate clothing. The format can be used in multi-segmented thermal models and can continue to be developed and improved as more information on wetted clothing properties become available.

Abreviations List:
A_D, Dubois area, body surface area, m^2; A_s, Wetted surface area of the spot m^2 ; A_b, Surface area of the body segment, could also be written as A_D if applied to the whole body, $m^{2,}$ clo, standard unit of thermal resistance for clothing 1 clo = 0.155 m^2·K/W; Cp_{bl}, Specific heat of blood, kJ/(kg·K); C_{sk}, Specific heat of the body's skin node, kJ/(kg·K); c_{sw}, Sweat rate coefficient, unitless; d, Subscript indicates part of the unsaturated, dry, clothing assumption heat and mass transfer, unitless; $E_{rsw,m}$, Modified form of ASHRAE regulatory sweat rate equation, W/m^2; E_{rsw}, Evaporation energy from latent heat transfer of regulatory sweat rate, W/m^2; $E_{sk,d}$, Energy exchanged between the environment and the skin's surface by sweat evaporation, W/m^2; E_s, latent energy transferred between the saturated spot and the environment, W/m^2; $EVAP_{mass}$, Mass evaporated from a thermal manikin, kg; E_x, Energy removed from the system at location x fabric, W; f_{cl}, Clothing area factor, unitless; h_c, Convective heat transfer coefficient, W/(m^2·K); h_e, Evaporative heat transfer coefficient, W/(m^2·Pa); h_{fg}, Latent heat of vaporization of sweat, kJ/kg; H_{heat}, Heat loss from the skin of a thermal manikin, W/(m^2·K); h_o, Operative heat transfer coefficient = h_r+h_c, W/(m^2·K); H_o, Sensible heat transfer between the environment location x in the fabric, W; H_s, Heat transfer by the body out to the environment at position x in Kerslake's formulation, W; h_r, Radiation heat transfer coefficient, W/(m^2·K); H_s, Heat removed from the clothing system, W/m^2; i, Time step iteration number, integer; i_m, Fabric permeability factor, unitless; K, Massless thermal conductivity between the skin and core segments, W/(m^2·K); k_1, Effective conductance to the environment to location x in the fabric, W/(m·K); k_2, Conductivity in the fabric from skin surface to location x in the fabric, W/(m·K); k_o, Overall conductance to the environment, W/(m·K); m_b, Mass of the body, kg; $\dot{m}_{rsw}$, Mass flow rate of regulatory sweat for thermoregulation, kg/s; m_s, Mass in wetted spot, kg; $m_{s,i}$, Mass in

wetted spot at time step, i, kg; $m_{s,i+1}$, mass of sweat in the spot at the next time step, i+1, kg; $\dot{m}_{s,in}$, mass of sweat entering the spot by not evaporating through the clothing, kg/s; $\dot{m}_{s,net}$, mass of sweat in the spot, kg/s; $\dot{m}_{s,out}$, mass of sweat leaving the saturated spot by evaporation, kg/s; ø, Relative humidity, %; P_o, Saturated pressure of operative environment, Pa; PPE, Personal Protective Equipment; $P_{sat}(T)$, Saturated pressure at temperature, T, Pa; P_x, Partial pressure at location x in the fabric, Pa; Q_{bl}, Volumetric flow rate of blood, m^3/s; $Q_{body,s}$, Conduction energy transfer between body an wet clothing, W/m^2; $Q_{C+R,d}$, Convection and radiation energy exchanged between the skin and the ambient through the dry, unsaturated clothing, W/m^2; $Q_{C+R,s}$, Energy exchange by the spot with the environment by way of convection and radiation, W/m^2; $Q_{evap,d}$, Latent energy exchanged between the skin surface through the dry, non-wetted clothing, W/m^2; $Q_{evap,s}$, Latent energy exchanged between the spot surface and the ambient, W/m^2; Q_{met}, Metabolic rate energy production, W/m^2; Q_{resp}, Energy exchange with the environment through respiration, W/m^2; Q_{shiv}, Shivering energy production, W/m^2; Q_{sktocr}, Energy exchange between the body skin and core elements of a two-node model, W/m^2; R_{cl}, Thermal resistance of the dry, unsaturated clothing, $(m^2 \cdot K)/W$; $R_{cl,w}$, Thermal resistance of the saturated clothing, $(m^2 \cdot K)/W$; Re_{cl}, Evaporative resistance, $(m^2 \cdot Pa)/W$; s, Subscript denotes part of the saturated spot area, unitless; $\dot{St}_{cr}$, Energy storage rate of the core note, W/m^2; $\dot{St}_{sk}$, Energy storage rate of the skin node, W/m^2; SW_{mod}, Sweat rate proportional gain term, unitless; SW_{tot}, Total sweat mass, kg; T_a, Ambient air temperature, K; T_b, mean body temperature, K; T_{bset}, mean body temperature set point, K; T_{cr}, Core body temperature, K; $T_{cr,i}$, Core body temperature at time step, i, K; TcoreHS, Core temperature of the human subjects, °C; TcoreTN, Core temperature predicted by the standard ASHRAE Two-Node Model, °C; TcoreTNM, Core temperature predicted by the modified ASHRAE Two-Node Model, °C; TN Evap Sweat, Sweat evaporation total predicted by the standard ASHRAE Two-Node Model, kg; TNM Evap Sweat, Sweat evaporation total predicted by the modified ASHRAE Two-Node Model, kg; T_o, Operative temperature, K; T_r, Mean radiant temperature of the environment, K; T_s, Surface temperature of the saturated spot of clothing, K; T_{sk}, Skin temperature, K; $T_{sk,i}$, Skin temperature at time step, i, K; T_x, Temperature at location x in the fabric, K ; SWHS, Sweat production of human subjects over the course of the experiment, kg; SWTN, Sweat production prediction by the standard ASHRAE Two-Node Model, kg; SWTNM, Sweat production prediction by the modified ASHRAE Two-Node Model, kg; v_a, air velocity, m/s; w_c, Saturated surface area percentage, unitless; x, distance inside the saturated material in the saturated fabric from the skin; α_{sk}, Core to skin body mass fraction ratio term, unitless; Δt, time period, s; ε_s, Heat exchange efficiency of the wetted spot, unitless; η_{sw}, Sweating efficiency, unitless; ρ_{bl}, density of blood, kg/m^3; ϕ_w, Fraction of sweat rate available to add to the spot, unitless

Keywords
wetted clothing; sweat; saturation; model validation; military ensemble; desert environment; core temperature; skin temperature; two-node model;

1.0 Introduction

Heat stress is a major limiting factor impacting the ability of humans to perform work, complete tasks, and engage in sports and recreation. Heat stress occurs when not enough energy is expelled from the body to the environment through the different modes of heat and mass transfer. In very harsh conditions these pathways can also enable the absorption of energy. The evaporation of sweat is crucial to the survival of human beings in high temperatures, wearing clothing and other garments impedes this critical function. The measure of this impediment is generally referred to as levels of evaporative

resistance, Re_{CL}. In extreme conditions, the ability to quantify and predict the evaporative resistance of an ensemble is essential for human thermal models.

In the current study, human trials in extreme environments were conducted and physiological performance was measured. Prior to conducting these studies, the dry and evaporative resistances of the clothing system were quantified with a thermal manikin and used in a predictive model. The human trial results were then compared to model predictions. The comparison revealed an important physical pathway for energy exchange was missing from the human thermal models, the effect of evaporative heat transfer from sweat-soaked clothing.

In human thermal models it is commonly assumed that evaporation takes place at the surface of the skin, and clothing is only factored in as an evaporative resistance that provides some barrier to moisture transport. Fundamental to most of these models, including the ASHRAE formulation of the two-node model in the work of Gagge et al. (1986); is the assumption that clothing does not wet or become saturated with sweat (ASHRAE, 2013; Gagge and Nishi, 1977; Stolwijk, 1971; Stolwijk and Hardy, 1966). In most situations where sweating is not excessive, such as office work, this assumption is very reasonable. However, if the sweat rate is greater than what can be evaporated to the environment, the saturated fabric becomes a site of heat and mass transfer in series with the skin, complicating the transfer equations from the simple resistance approach. The model presented later corrects this simple approach.

There have been numerous studies into, and explanations provided for, heat and moisture transport through fabric. Hardy (1950) provides one of the first reviews of works discussing evaporation from the surface of the body drawing on the works of Büttner, Gagge, Benedict, Hardy, DuBois, and Winslow. These authors primarily describe the effects of evaporation with the non-wetting clothing assumptions where fabric evaporative resistance impedes the water vapor flow due to the partial pressure difference. The permeability factor, i_m, was introduced and allowed the sensible heat loss to be approximately related to the insensible heat loss (Woodcock, 1962a, b).

There are also examinations in the literature of the transient effects of adsorption and desorption of water vapor and the resultant effects on thermal comfort. Lotens (1993) provides an in-depth description of clothing adsorption and desorption including a discussion of 2-layer clothing expanding on the work of Jones (Jones and Ogawa, 1992; Jones and Ogawa, 1993). In these studies, the moisture transport at the surface of the clothing did not completely saturate the fabric, and the moisture was deposited by adsorption, desorption, evaporation, and condensation. Lotens (1993) briefly covers saturating garments in an unlikely adsorption case under otherwise compensable conditions. and Other authors have readdressed the sorption-desorption of water vapor in fiber and its effects on thermal capacity and fabric conductivity (Yi et al., 2004).

Fourt and Harris discuss the use and results of an instrumented, wetted cylinder in crossflow empirically determining fabric properties (Fourt and Harris, 1950). They also cover the “inertia effect” inherent in clothing stemming from the capacity of the fibers to absorb moisture even without liquid water being present, similar to the adsorption and desorption previously discussed by Lotens (1993), Jones and Ogawa (1992), and Jones and Ogawa (1993). They point out that some or all of the evaporative cooling at the surface of the skin will be effectively cancelled out by the adsorption in the clothing, which also causes a lag in cooling applied to the body through evaporation.

Kerslake (1972) is cited as developing the first efficiency equations for evaporation from saturated clothing. This theoretical framework of evaporation efficiency was used by Wang et al. (2013) and Wang

et al. (2014) to formulate an evaporation efficiency of wet clothing. Tests were conducted under isothermal conditions with the clothing and skin in direct contact thus T_o=T_{sk} . Heat loss from the skin of the manikin H_{heat} and based on the actual mass evaporated as measured by a scale, $EVAP_{mass}$, define the efficiency. Wang et al. determined this efficiency value for four different types of fabrics in direct contact with the skin. They used the equivalent efficiency value from Havenith et al. (2008) where the $EVAP_{mass}$ term was further split to account for the sweating efficiency, η_{sw} out of the sweat total SW_{tot}.

The current models are insufficient in describing cases where the clothing is not in constant contact with the skin and is saturated with excess, dripping sweat either by periodic touching or wicking from constant-contact body points (e.g. armor and equipment). An approach similar to that used by Kerslake is used in this study; however, the problem is formulated based on the surface area of clothing saturated and not on the moisture penetration thickness.

2.0 Methods

2.1 Saturated clothing model correction

The models described in the previous section are insufficient when the clothing is both not in constant contact with the skin and is saturated with excess, dripping sweat by periodic touching or wicking from constant contact body points. A formulation of the basic heat tranfer problem is presented in this section for a saturated spot on clothing. A general energy balance is applied to the wet fabric where the energy lost to the environment and cooling provided to the body is defined. Next, an efficiency of the saturated area is developed based on the calculated energy balance and then the wet fabric model is expended into a partially wet/dry body heat loss model. Once formulated, this research is integrated into the simplified 2-node model from ASRHAE and validated against an experimental data set from subjects working in hot and dry conditions (Elson et al., 2013; Gagge et al., 1986).

The evaporation from the wetted clothing area occurs at the surface of the clothing, not the skin, as with the non-wetting clothing assumption. To account for the influence of the body temperature and environment, an energy balance is performed on the fabric between the energy from the body and the spot, $Q_{body,s}$, energy from the evaporation of the spot, Q_{evap}, , and energy from convection and radiation on the spot, $Q_{C+R,s}$, shown in Figure 1 and in Equation (1), assuming steady state.

$$\mathbf{0} = \boldsymbol{Q_{body,s}} + \boldsymbol{Q_{evap,s}} + \boldsymbol{Q_{C+R,s}} \quad \textbf{(1)}$$

The fabric and liquid are assumed to be a massless node; therefore, the energy balance from Equation (1) can be written using the values below in Equation (2). In this new equation, T_s is the surface temperature of the spot, $R_{cl,w}$ is the thermal resistance between the wetted spot and the skin, f_{cl} is the clothing area factor, h_c is the convective heat transfer coefficient, $P_{sat}(T)$ is the partial saturated pressure at some temperature T, the dry air temperature is T_a, the evaporative heat transfer coefficient is h_e, the radiation heat transfer coefficient is h_r, and T_r is the mean radiant temperature.

$$\mathbf{0} = \frac{\boldsymbol{T_{sk}} - \boldsymbol{T_s}}{\boldsymbol{R_{cl,w}} + \frac{\mathbf{1}}{\boldsymbol{f_{cl}h_c}}} + \frac{\boldsymbol{P_{sat}}(\mathbf{T_s}) - \boldsymbol{P_{sat}}(\boldsymbol{T_a})\boldsymbol{\phi}}{\frac{\mathbf{1}}{\boldsymbol{f_{cl}h_e}}} + \boldsymbol{h_c f_{cl}}(\boldsymbol{T_a} - \boldsymbol{T_s}) + \boldsymbol{h_r f_{cl}}(\boldsymbol{T_r} - \boldsymbol{T_s}) \quad \textbf{(2)}$$

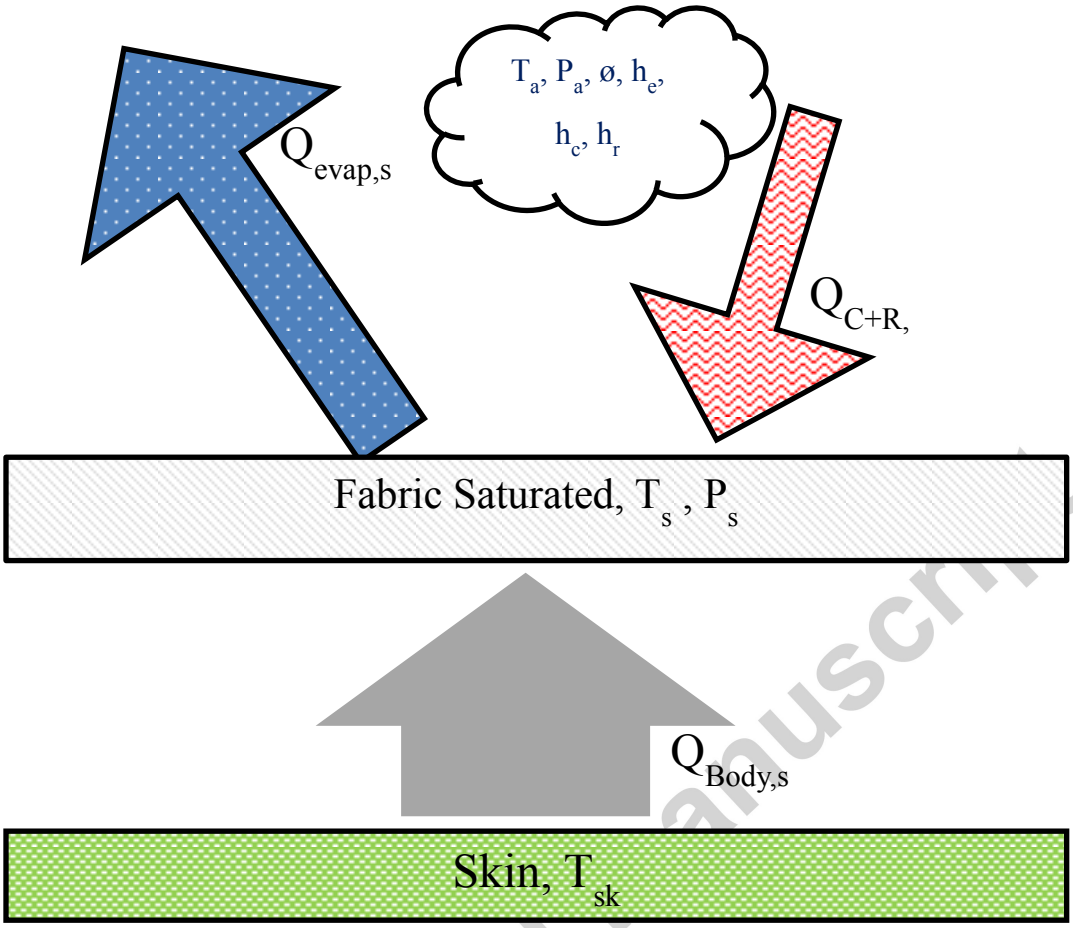

Figure 1 Energy balance at the surface of the clothing for a saturated fabric. In this figure starting from the skin surface: T_{sk} is the temperature of the skin, Q_{body} is the heat transfer between the body surface and the saturated fabric. A resistance between the wetted fabric and the skin, $R_{cl,w}$, exists with some combined convection and radiation on the fabric surface Q_{C+R}. The other term interacting with the wetted fabric surface at temperature T_s and partial pressure P_s, is the evaporation component $Q_{evap,s}$.

Figure 1 shows energy balance on the wetted fabric spot that is evaluated in Equation (2). This energy balance is similar to that presented by Kerslake (1972); however, in this work the radiation and convection effects have been included and, ultimately, $Q_{body,s}$ is needed to balance the equation. The cooling efficiency is that of the evaporation from the 100% wetted spot, $Q_{evap,s}$, not the relative loss of efficiency of evaporation from the uncovered skin surface, as described in the second term of Equation (2) and instead is replaced with Equation (3).

$$\boldsymbol{\varepsilon_s(T_s)} = \frac{\boldsymbol{Q_{body,s}}}{\boldsymbol{Q_{evap,s}}} = \frac{\dfrac{\boldsymbol{T_{sk} - T_s}}{\boldsymbol{R_{cl,w}}}}{\boldsymbol{h_e \cdot (P_{sat}(T_a) \cdot \phi - P_{sat}(T_s))}} \quad \textbf{(3)}$$

This equation is solved numerically to find the temperature of the fabric surface and calculate the heat exchange efficiency of the wetted spot, ε_s. Properties and boundary conditions can be seeded from previous iterations for transient simulations or averaged over the course of the test depending on the resolution desired and knowledge of actual conditions. The efficiency of the spot is calculated from the

fraction of the energy removed from the body over the energy removed from the wetted surface by evaporation using the calculated wetted fabric temperature.

The evaporation from a surface of the simulated human can now be defined with the saturated and dry clothing areas, Figure 2, governed by the saturated surface area percentage, w_c, in Equation (4).

$$\boldsymbol{Q_{evap} = (1 - w_c) \cdot E_{sk,d} + \varepsilon_s \cdot w_c \cdot E_s} \quad \textbf{(4)}$$

The convection and radiation terms are taken into account at the fabric surface in the saturated fabric area, the area for convection and radiation exchange by the non-saturating method must also be scaled by w_c as shown in Equation (5) The introduction of the latent heat transfer from the dry area is presented in a new notation, $E_{sk,d}$ which is equal to $Q_{evap,d}$, and in ASHRAE is given as E_{sk}. This work uses the subscript 'd' to denote the dry fabric assumption and the subscript 's' to denote the saturated spot. Also included is the combination of the convective and radiation heat exchange term for the non-saturation assumption, $Q_{C+R,d}$, which is equivalent to the C+R term from ASHRAE, but has been changed to a subscript in order to avoid confusion with standard units (Gagge et al., 1986).

$$\boldsymbol{(1 - w_c) \cdot [Q_{C+R,d} + E_{sk,d}]} \quad \textbf{(5)}$$

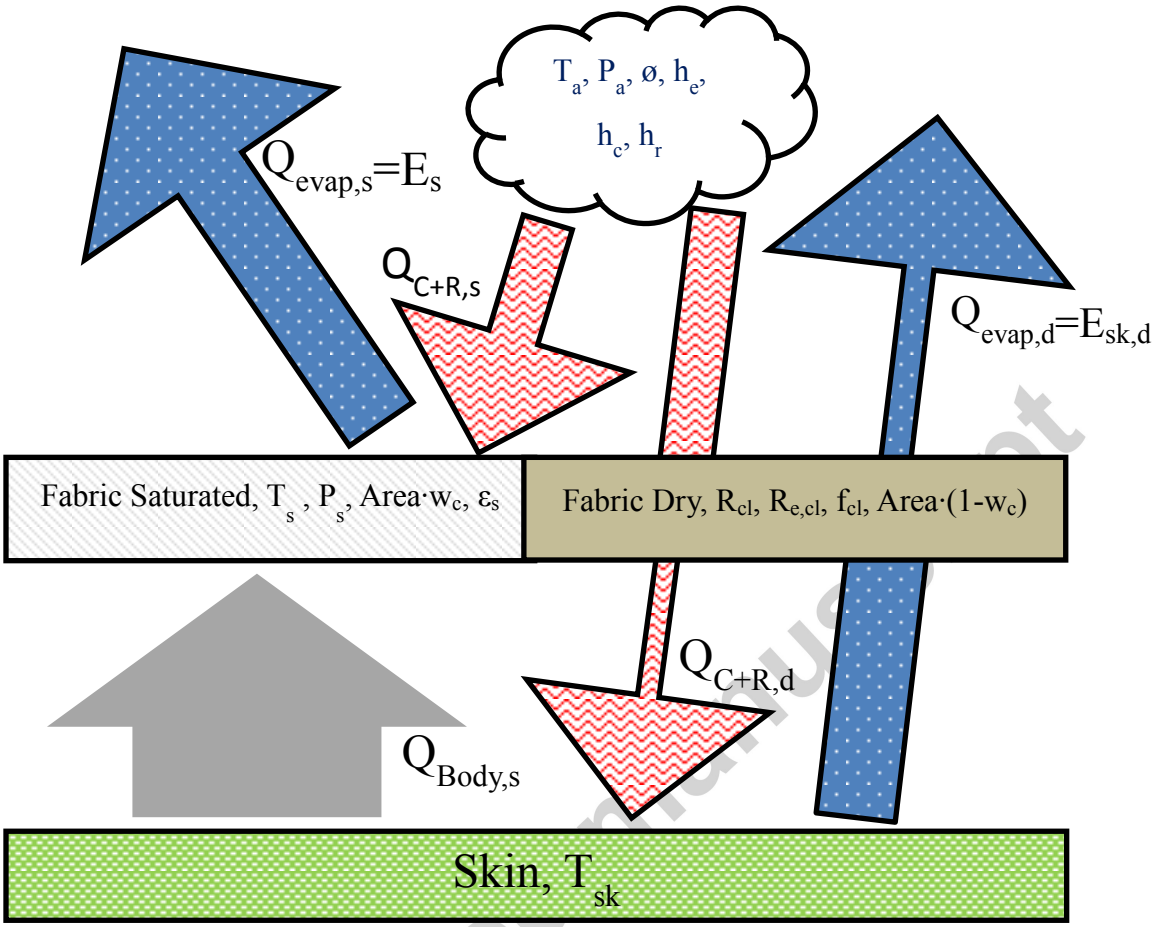

Figure 2 Energy transfer for a skin node using the saturated area and non-wetting clothing assumption acting in parallel through two different energy transport formulas. The total surface is split up with the fractional term w_c representing the percent of the surface that is saturated. On the left side of the figure the saturated fabric pathway is represented where Equations (2) and (3) were used to determine the efficiency of the spot, ε_s, under assumed conditions to account for the iterative energy balance at that node. The energy exchanged with the environment in this case is $Q_{body,s}$ which interacts with the saturated fabric at temperature T_s, partial pressure P_s, over the surface area, A_b, multiplied by the fractional wetted area. $Q_{C+R,spot}$ is calculated in Equation (2) along with the $Q_{evap,\,spot}$, which serves as the bridge between the two equations. The dry side of the fabric employs the standard method used in the ASHRAE model (Gagge et al., 1986) where the clothing has thermal resistance, R_{cl}, evaporative resistance, $R_{e,cl}$, clothing area factor, $f_{cl,}$ over the area in question, A_b, multiplied by the fraction uncovered by the wetted spot. Q_{C+R} is the sensible heat transfer through the clothing from the skin at temperature T_{sk} and the environment, and $Q_{evap,skin}$ is the latent heat transfer component to the non-wetting skin. The environment is at the air temperature T_a, partial pressure, P_a, relative humidity ø, and interacts with the saturated area through the evaporative heat transfer coefficient h_e, convective heat transfer coefficient h_c, and linearized radiation heat transfer coefficient h_r.

An experiment was run to develop a relationship between liquid spot mass and the surface area. An impermeable layer was placed behind the uniform fabric to ensure all the liquid entered the clothing, and a titration burette was used to apply a defined quantity of water to a single layer of the subject ensemble material on a flat surface. The size of the saturated area was mathematically represented as shown in Figure 3 with two semicircles and a rectangle to account for any lack of symmetry.

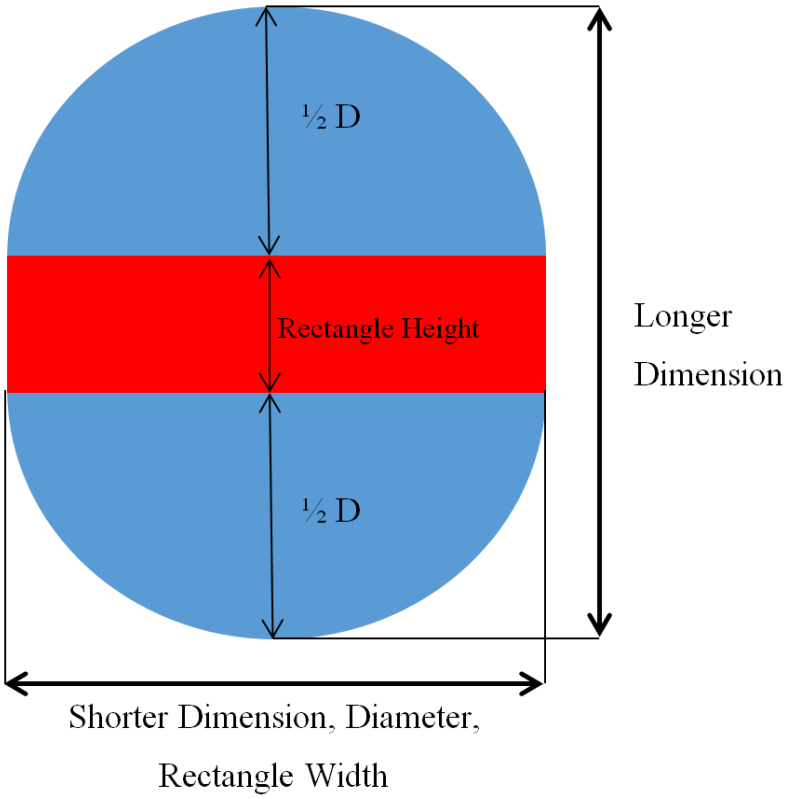

Figure 3 Method of calculating saturated area for each unit of mass is shown here to demonstrate the calculation of area from Figure 4. When the surface was wetted, the spot which was created was usually not perfectly circular. Therefore it was assumed to be two semi circles with a rectangular area in between. This allowed dimensions to be measured using a rectangular set of coordinates and simplified measurement. Ideally the fabric would wick uniformly from the center forming a circle; however this was not usually the case.

The results of nine different mass-to-area measurements are shown in the plot and linear approximation of Figure 4. This equation provides the area saturation, $A_{w,}$ per mass of water for this fabric, m_s, in Equation (6). The formula for the percentage of the surface covered by the spot is given by dividing the saturated area, $A_{s,}$ by the available surface area of the body segment, A_b, in Equation (7). The fabric used to calculate these parameters was the pants of the military ensemble worn by the human subjects in this evaluation, the material of which was similar to the sleeves of the uniform blouse worn. The mass-to-area ratio is likely dependent on a number of parameters including the material composition, type of yarn, weaving pattern, thickness, and other adsorption and adsorption properties. It will likely be necessary to measure the mass-to-area ratio for each fabric when using this method in practice.

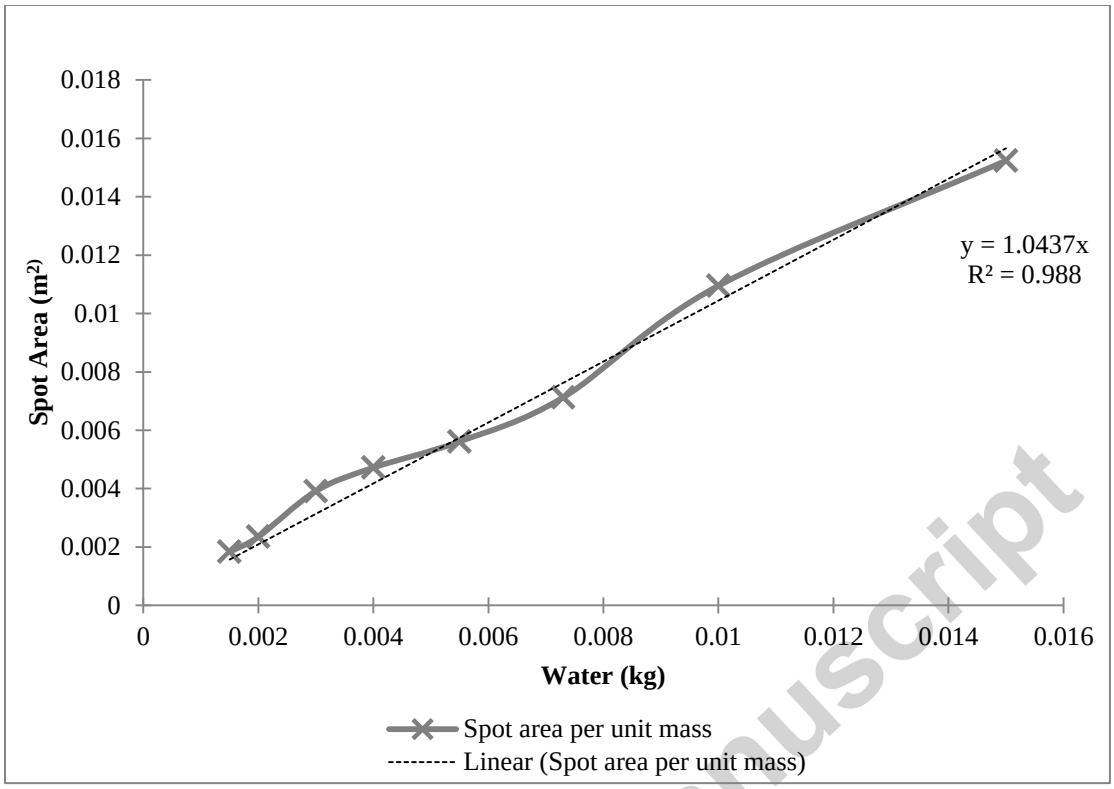

Figure 4 Spot Area vs. Absorbed Mass graph and linear regression

$$\boldsymbol{A_s = m_s * 1.0437 (m^2/kg)} \quad \textbf{(6)}$$

$$\boldsymbol{w_c = A_s / A_b} \quad \textbf{(7)}$$

Next, the mass balance of the excess sweat is formulated for each segment. The standard equation from the ASHRAE model (Gagge et al., 1986) for the potential energy removed by all of the sweat produced, assumed without wetting clothing or dripping, is given in Equation (8), where E_{rsw} is the evaporation energy composed of the latent heat of vaporization, h_{fg}, and regulatory sweat rate, $\dot{m}_{rsw}$.

$$\boldsymbol{E_{rsw} = \dot{m}_{rsw} \cdot h_{fg}} \quad \textbf{(8)}$$

However, the evaporative resistance of the fabric, coverage area, relative humidity, and evaporative heat transfer coefficient determine the amount of sweat that can be evaporated. In energy terms from the work of Gagge et al. (1967) this is given as, E_{sk}, and in this notation as $E_{sk,d}$ and $Q_{evap,d}$ for some surfaces shown in Equation (9).

$$\boldsymbol{E_{sk,d} = \frac{P_{sat}(T_{sk}) - P_{sat}(T_a)\phi}{R_{e,cl} + \frac{1}{f_{cl} h_e}}} \quad \textbf{(9)}$$

The mass available to enter the spot per unit time, $\dot{m}_{s,in}$ is shown in Equation (10) and is the leftover sweat that did not evaporate. It is possible that some of the sweat does not evaporate, drips, or does

not penetrate garments or equipment; therefore, an efficiency, φ_w, is used to account for this trapped or lost liquid mass.

$$\dot{m}_{s,in} = \varphi_w \cdot \frac{E_{rsw} - (1 - w_c) \cdot E_{sk,d}}{h_{fg}} \quad (10)$$

The differential mass balance is shown in Equation (11), where $\dot{m}_{s,out}$, is the mass leaving the saturated clothing area by evaporation shown in Equation (12). The latent energy removed from the spot to provide evaporation is given by E_s, shown in Equation (13) and is the mass removed multiplied by the latent heat.

$$\frac{dm_s}{dt} = \dot{m}_{s,net} = \left(\dot{m}_{s,in} - \dot{m}_{s,out}\right) \quad (11)$$

$$\dot{m}_{s,out} = \frac{w_c \cdot E_s}{h_{fg}} \quad (12)$$

$$E_s = \frac{P_{sat}(\mathrm{T}_{sk}) - P_{sat}(T_a)\phi}{\frac{1}{f_{cl} h_e}} \quad (13)$$

If this method is to be applied to numerical simulations, the differential equation must be discretized. To accomplish this, the saturated area contains mass which must be conserved at a given time step, *i*, separating the next iteration by some time period, Δt. The net mass flow rate entering or leaving the spot, $\dot{m}_{s,net}$, from Equation (11), multiplied by the time step and added to the spot mass at the current time step, $\dot{m}_{s,i}$, yields the mass of the saturated area for the next time step, $\dot{m}_{s,i+1}$, Equation (14). Obviously, language must be included to ensure proper signs and that the spot cannot result in a negative mass according to the chosen method of programing.

$$m_{s,i+1} = m_{s,i} + \dot{m}_{s,net} \cdot \Delta t \quad (14)$$

It is also likely that the sweat production will not match empirically-derived equations in this case, but maintaining the correct sweat mass balance is extremely important. It is relatively common in the literature, and called for in the ASTM standards, to measure the mass of the nude subjects at the beginning and end of the test to determine the total mass lost due to sweat (ASTM, 2010). Therefore, this known quantity can be used to inform the mass and energy balance of the body. If the clothing and equipment masses before and after are measured, and dripping is minimized, this can further be used to enhance model effectiveness; however, only the nude measurement of the subjects was performed in the validation experiments. In this model, the sweat rate production term of each subject is scaled through the use of a proportional term, SW_{mod}, until the simulated sweat total is equal to the measured sweat produced by the human subject. A purely proportional gain factor may not account for time effects, but it is a functional approximation for the type of data generally available. Adding the sweat rate gain factor to the sweat rate equation produces a modified regulatory sweat rate, $E_{rsw,m}$, in Equation (15). In future use it would be ideal to develop a time-dependent gain factor or a more accurate sweat model.

$$E_{rsw,m} = SW_{mod} \cdot \dot{m}_{rsw} \cdot h_{fg} \quad (15)$$

This model can be scaled and employed on any surface that has sufficient area to allow the spot to form. Therefore, it can be used on segmental models such as those by Fiala (Katić et al., 2016), Stolwijk

(Stolwijk, 1971; Stolwijk and Hardy, 1966), or on two-node models such as the easily assessable ASHRAE (2013) model, as will be demonstrated.

2.2 Model Implementation

The standard ASHRAE equation was used with the exception of the boundary condition and sweat rate terms, those being modified in this model to include the saturated area. The energy balance on the skin node is given in Equation (16) in the notation of this paper, balancing the energy from the core to the skin, Q_{sktocr}, with the evaporation transfer and the convective and radiation transfers, $Q_{C+R,d}$. Any energy increase or decrease becomes part of the storage term, $\dot{St}_{cr}$, for the skin, resulting in a temperature change.

$$\mathbf{0} = \boldsymbol{Q_{sktocr}} + \boldsymbol{Q_{evap,d}} + \boldsymbol{Q_{C+R,d}} + \boldsymbol{\dot{St}_{sk}} \tag{16}$$

Similarly, the energy balance of the core is shown in Equation (17) and the energy terms in order are the metabolic rate, Q_{met}; shivering, Q_{shiv}; energy exchange from the core to the skin, Q_{crtosk}; respiration losses, Q_{resp}; and any energy storage in the core, $\dot{St}_{cr}$. Thus, the temperature of the segment can be calculated. As this model only deals with the external boundary conditions of the body, only the skin energy balance will be discussed.

$$\mathbf{0} = \boldsymbol{Q_{met}} + \boldsymbol{Q_{shiv}} + \boldsymbol{Q_{crtosk}} + \boldsymbol{Q_{resp}} + \boldsymbol{\dot{St}_{cr}} \tag{17}$$

The ASHRAE model sweat rate term is given in Equation (18) where c_{sw} is the sweat rate coefficient, T_b is the mean body temperature, and T_{bset} is the mean body set point temperature .

$$\dot{\boldsymbol{m}}_{\boldsymbol{rsw}} = \boldsymbol{E_{rsw}} \cdot \boldsymbol{h_{fg}} = \frac{\boldsymbol{c_{sw}} \cdot (\boldsymbol{T_b} - \boldsymbol{T_{bset}}) \cdot \exp\left[\frac{\boldsymbol{T_{sk}} - \mathbf{34^{o}C}}{\mathbf{10.7}}\right]}{\boldsymbol{h_{fg}}} \tag{18}$$

The ASHRAE model relies on the same boundary condition calculations for the singular skin node evaporation from Equation (9) and conduction and radiation $Q_{C+R,d}$ in Equation (19) (Gagge et al., 1986).

$$\boldsymbol{Q_{C+R,d}} = \frac{\mathbf{T}_{\boldsymbol{sk}} - \boldsymbol{T_o}}{\boldsymbol{R_{cl}} + \frac{\mathbf{1}}{\boldsymbol{f_{cl}} \boldsymbol{h_o}}} \tag{19}$$

Finally, the energy balance of the skin node can be written for the new skin temperature as shown in Equation (20). This equation includes the ASHRAE Model, evaporation though the dry clothing energy term, $E_{sk,d}$. The model contains a number of physiological parameters, the constants of which are found in the reference. The core to skin body mass ratio is α_{sk}, T_{cr} is the core body temperature, K is the massless thermal conductivity between the skin and core segments, ρ_{bl} is the density of blood, Q_{bl} is the blood volumetric flow rate, C_{sk} is the specific heat of the skin node, m_b is the mass of the body, and A_D is the surface area of the body or Dubois Area, and Cp_{bl} is the specific heat of blood (Gagge et al., 1986).

$$\frac{\boldsymbol{d}(\boldsymbol{Tsk}\frac{\boldsymbol{\alpha_{sk}} \cdot \boldsymbol{m_b} \cdot \boldsymbol{C_{sk}}}{\boldsymbol{A_D}})}{\boldsymbol{dt}} = -\left[[\boldsymbol{Q_{C+R,d}} + \boldsymbol{E_{sk,d}}] + (\boldsymbol{K} + \boldsymbol{\rho_{bl}} \cdot \boldsymbol{Q_{bl}} \cdot \boldsymbol{Cp_{bl}}) \cdot (\boldsymbol{T_{cr}} - \boldsymbol{T_{sk}})\right] \tag{20}$$

Implementing the saturated area spot model involves a number of modifications to the single node ASHRAE model already described (Gagge et al., 1986). The first is including the modified energy version of the sweat rate $E_{rsw,m}$ as shown in Equation (21).

$$\boldsymbol{E_{rsw,m} = SW_{mod} \cdot c_{sw} \cdot (T_b - T_{bset}) \cdot \exp\left[\frac{T_{sk} - 34^{o}\mathrm{C}}{10.7}\right]} \quad \textbf{(21)}$$

The second area includes the mass balance equations described in Equations (10), (11), (12), (13), and (14), incorporating all of the skin surface area and sweat into the uniformly distributed model. The efficiency equation can be developed for ε_s from Equation (3). The E_s energy value from the spot needs to be added and a value decided on for the available sweat φ_w described in Equation (10). Finally, an empirically described equation for the mass-per-surface area value needs to be determined for the fabric(s) used and an area wetting coefficient, w_c, created.

This can be included into the iterative energy balance equation for the skin node, Equation (20), becoming Equation (22). The standard ASHRAE two-node model skin node equation now contains the additional terms of the spot efficiency, percentage area covered, and energy term from Equation (4). The other modification made to the two-node model is accounting for the new surface area percentage that uses the non-wetting clothing assumption from Equation (5) combined with the two-node skin energy equation separated for time-step skin temperature iteration, i. This includes the addition of the core temperature at time step 'i',$T_{cr,i}$ and skin temperature at time step 'i', $T_{sk,i}$.

$$\frac{d\left(Tsk\frac{\alpha_{sk} \cdot m_b \cdot C_{sk}}{A_D}\right)}{dt} = -\left[(1 - w_c) \cdot [Q_{C+R,d} + E_{sk,d}] + \varepsilon_s \cdot w_c \cdot E_s + (K + \rho_{bl} \cdot Q_{bl} \cdot Cp_{bl}) \cdot (T_{cr,i} - T_{sk,i})\right] \quad \textbf{(22)}$$

2.3 Testing Data

A study performed on 24 U.S. Army soldiers , 22 men and 2 women, at the Institute for Environmental Research (IER), Kansas State University simulating midday, summer conditions in the Middle East (Elson and Eckels, 2015), was used to validate the model presented above using 21 of the subject's resuts. Data necessary for comparison with the tool was not gathered from 3 subjects, who were excluded.

Figure 5 Human subject testing at the Institute for Environmental Research at Kansas State University

The environmental conditions were set at 42.2 ºC dry air temperature, T_a; 54.4 ºC mean radiant temperature, T_r; 20% relative humidity, ϕ; and an air velocity of 2.0 m/s, v_a. The subjects walked on treadmills in the environmentally controlled chamber with a targeted metabolic rate of 375-400W. Metabolic rate was estimated through the use of the equations presented by Pandolf et al. (1977), which predicted walking velocity based on targeted metabolic rate. The walking rate was refined or verified by use of a VO_2 machine on each subject. Skin temperature was measured at seven locations using calibrated Type-T thermocouples and core body temperature was recorded using CoreTemp® ingestible temperature pills and recorders. The subjects were weighed before and after the experiment wearing only the standard boxer briefs to determine mass loss due to sweat. Any water consumed during the test was measured and added to the mass loss figure and no urine was excreted in any of the tests.

The subjects were allowed to drink approximately body temperature water at 37 ºC ad libitum and were required to drink at least 250 mL every 30 minutes during the test to prevent dehydration. The subjects were active-duty soldiers wearing a base ensemble of athletic shoes, cotton socks, cotton boxer-briefs, Flame Retardant (FR) Battle Dress Uniform (BDU) trousers, FR Army Combat Shirt (ACS), cotton/nomex gloves, Soldier Plate Carrier (SPC) armor system, and Army Combat Hemet (ACH). The thermal and evaporative resistances for the ensemble were measured on a 20-zone Newton thermal manikin (Thermetrics, USA) according to ASTM 1291 and ASTM 2370 (ASTM, 2016a, b). The intrinsic thermal resistance of the ensemble was 0.155 m^2ºC/W (1.00 clo) and the evaporative resistance was 26.2 (m^2Pa)/W and the clothing area factor was estimated to be 1.33.

The clothing completely covered the surface of the soldiers leaving only the face and neck exposed, therefore saturation of the fabric was the likely pathway for any excess sweat. Any risks to the subjects proposed in testing were reviewed and deemed minimal enough to be safe by both the university and military institutional review boards.

2.4 Simulation Results

This model was programmed using a set of measured and estimated boundary conditions taken from the human-subject experiments and is detailed in this section. The whole-body walking convection coefficient was estimated from the work of Danielsson (1993). To demonstrate the necessity for a

modified model to account for sweat saturation, the unmodified ASHRAE two-node model is presented first (Gagge et al., 1986).

Table 1 Baseline data comparison: Two-Node Model (TN) vs. Human Subject (HS). TcoreHS is the core temperature of the human subjects, TcoreTN is the core temperature predicted by the standard ASHRAE Two-Node Model, SWHS is the Sweat production of human subjects over the course of the experiment, and SWTN is the sweat production prediction by the standard ASHRAE Two-Node Model.

Subject	TcoreHS	TcoreTN	TcoreTN-TcoreHS	SWHS	SWTN	SWTN-SWHS	TN Evap Sweat
#	ºC	ºC	ºC	kg	kg	kg	kg
Average of subjects*	38.17	39.49	1.310	2.280	1.992	-0.288	0.962
Standard Deviation of Average of Subjects	0.482	0.463	0.557	0.434	0.336	0.409	0.106
Average Subject**	38.17	39.48	1.300	2.280	2.059	-0.222	1.090

**The Average Subject takes the average of all parameters from the 21 subjects and creates a single, representative subject.
*The Average of subjects is the average of 21 individual simulations, one for each human subject with sufficient data.

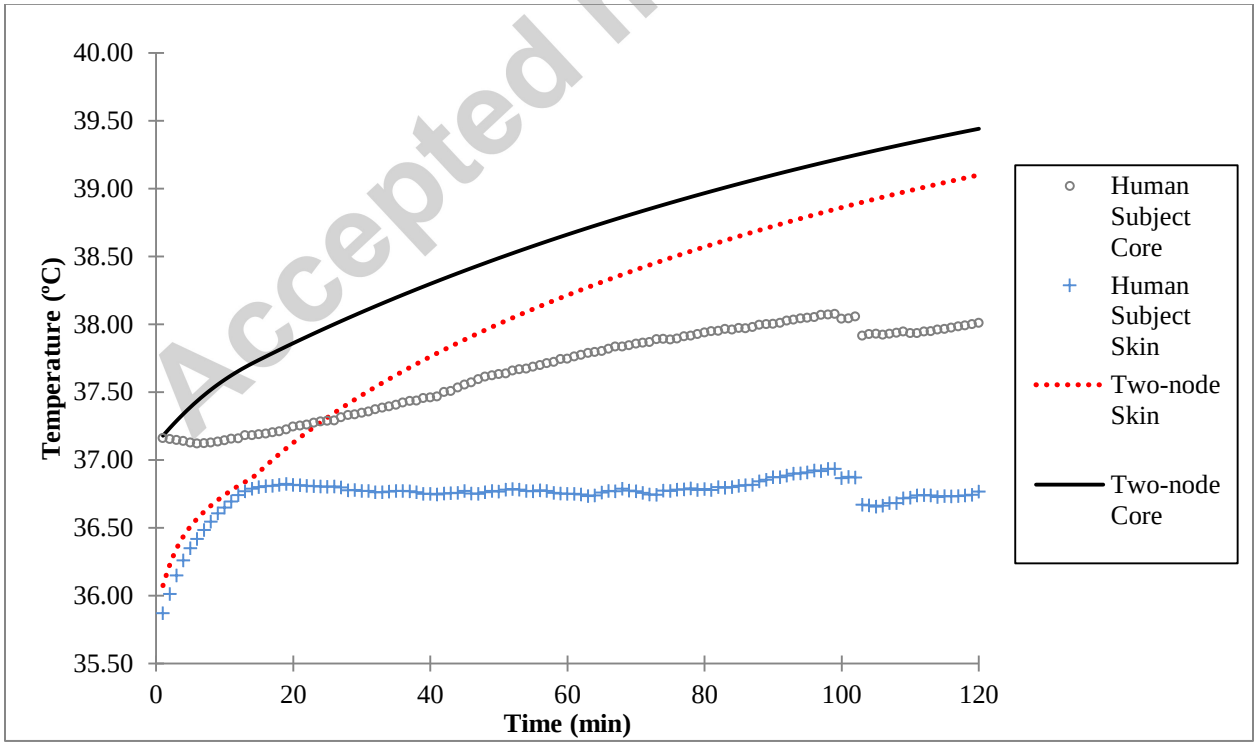

Figure 6 Core temperature comparison graph between the Average Subject Two-Node Model (TN) and the average Human Subject empirical data from 21 subjects, (HS)

Experimental data with the predictions of the unmodified ASHRAE model are shown in Table 1 and Figure 6. The Average of Subjects represents the average of each individual subject being modeled with the two-node model and also the average and standard deviations of those results. The test conditions prevented a total of eight subjects from finishing the full 120 minutes of the experiment for various reasons. Enough experimental data was acquired from five of these participants to simulate their individual performance using the models. Table 1 compares the final core temperature for each subject and the model is run using the parameters of each participant only for the time they remained in the test. This time effect can be observed in the human subject graphs of Figure 1 where subjects with higher skin and core temperatures leave the average around the 100 minute mark, lowering the average slightly. The Average Subject in Table 1 and Figure 6 takes the initial conditions and physical parameters such as weight, Dubois area, met rate, etc. and creates one average representative subject. As a result it doesn't have a standard deviation.

It is clear that the standard two-node model did not properly predict neither core or skin temperatures as expected. The two-node model prediction also shows that the overall sweat produced by the simulated human subjects was close to that of the empirical results, -0.288 ± 0.4097 kg, despite the poorly predicted core and skin temperatures. Finally, in the model the skin wettedness reaches 100%, w=1, almost immediately.

The inherent simplicity of the two-node model makes tradeoffs that could create potential errors in addition to, or compounding, the non-wetting clothing assumption. The average surface conditions in the two-node model means that different coverage areas, varying local clothing layers, and local environmental boundary conditions are not specifically addressed. The studied case is somewhat simplified because, based on interviews, in this high temperature military application the soldiers wear as little extra clothing as possible, usually one layer with a general maximum of two. The ensemble pieces that add extra layers are the underwear, socks, and the armor and pads. The armor and pads are relatively to completely vapor-impermeable and could create significant local effects, although this is averaged into the overall clothing properties by the thermal manikin when used in the two-node model. There are also different environmental boundary conditions in this analysis which could hypothetically play a role. However, there is not a significant difference in local skin temperatures when the subjects are in uncompensable conditions.

This leaves the largest mechanism for energy removal in this case, evaporation of sweat. The data set that the two-node model was based on used the information from Stolwijk (1971), which tested men exercising in the heat in "minimal clothing"; i.e. athletic shorts and shoes. In this case the body area covered by the clothing is minimal so any wetting effects could be ignored and sweat would drip freely as is assumed in the model. In the current study, any dripping sweat would be absorbed into the encapsulating ensemble, worn in part to protect the dismounted soldier from flames and flash burns, and therefore covers as much of the bare skin as possible. Except for the sweat leaving the body by the face, or evaporating through the clothing, the rest of the sweat is expected to be absorbed by the ensemble. This sweat will evaporate to the environment if the boundary conditions permit. Therefore, it should also be noted that the sweat produced by the two-node model is remarkably similar to that of the human subjects, despite the high core and skin temperatures. It is also likely that the two-node-model sweat rate is incompatible with the uncompensable heat-stress conditions found in this test.

To correct this assumption, the two-node model will be modified by adding the effect of evaporation from wetted clothing. The new model employing the more representative boundary conditions is

expected to perform much better. When applying the saturated clothing model, the three values required were the sweat rate modification term, the saturated-area-to-mass function for the fabric, Equation (6), and the calculation of the efficiency term between the fabric and the environment. In this case, based on the measured surface area of the body armor, 32% of the body surface area was considered impermeable. Therefore, φ_w, is set at 68% to account for the sweat absorbed and stored under the impermeable body armor. Similarly, the results from Figure 4 provide the empirical equation to be used to determine the saturated surface area percentage, w_c. Finally, to calculate the efficiency, an average skin temperature was used as the outside conditions were constant and the skin varied by < 2°C.

The following values were used in setting the boundary conditions for the thermal model: Ta = 42.2 ºC, T_r = 54.4 ºC, R_{cl}, w = 0.0443, T_{sk} = 36.7 ºC, h_r = 4.7 W/(m^2·K), h_c = 17.37 W/(m^2·K), h_e = 0.29793 W/(m^2·Pa), h_t = 22.069 W/(m^2·K), Relative Humidity = 20%. Plugging the values into the iterating energy balance of Equation (2) yielded the expected skin temperature of 27.4 ºC and a saturated area efficiency of 35% from Equation (3).

$$\boldsymbol{\varepsilon_s(T_s = 27.4\ ^{o}\mathrm{C}) = \frac{Q_{body}}{Q_{evap,s}} = \frac{\frac{T_{sk} - T_s}{R_{cl,w}}}{h_e \cdot (P_{sat}(T_a) \cdot \phi - P_{sat}(T_s))} = 35\%} \quad \textbf{(23)}$$

This new modified two-node model, with more appropriate boundary conditions, is compared to the measured results from human subject testing. The results of the average subject are shown in Table 2.

Table 2 The results comparing the modified two-node model (TNM) to the measured human subject results (HS). TcoreHS is the core temperature of the human subjects, TcoreTNM is the core temperature predicted by the modified ASHRAE Two-Node Model, SWHS is the Sweat production of human subjects over the course of the experiment, SWTNM is the Sweat production prediction by the modified ASHRAE Two-Node Model.

Subject	Tcore HS	Tcore TNM	TcoreTNM -TcoreHS	SWHS	SWTN	SWTNM -SWHS	TNM Evap Sweat	SWmod
#	ºC	ºC	ºC	kg	Kg	kg	kg	kg
Average of subjects*	38.17	38.33	0.150	2.280	2.280	0.000	1.570	1.830
Standard Deviation of Average of Subjects	0.482	0.473	0.383	0.434	0.434	0.006	0.270	0.705
Average Subject**	38.17	38.24	0.070	2.280	2.387	0.107	1.740	1.830

*The Average of subjects is the average of 21 individual simulations, one for each human subject with sufficient data.
**The Average Subject takes the average of all parameters from the 21 subjects and creates a single, representative subject.

Figure 7 displays the results of the simulation of the average subject compared to the human subject results. The results in Table 2 show that the average core temperature deviation from the human subject results at the end of the two-hour test is 0.07 ºC for the average subject. This is a much improved value compared to the original two-node mode. Furthermore, Figure 7 clearly shows the improvement in skin and core temperature predictions over the original two-node model.

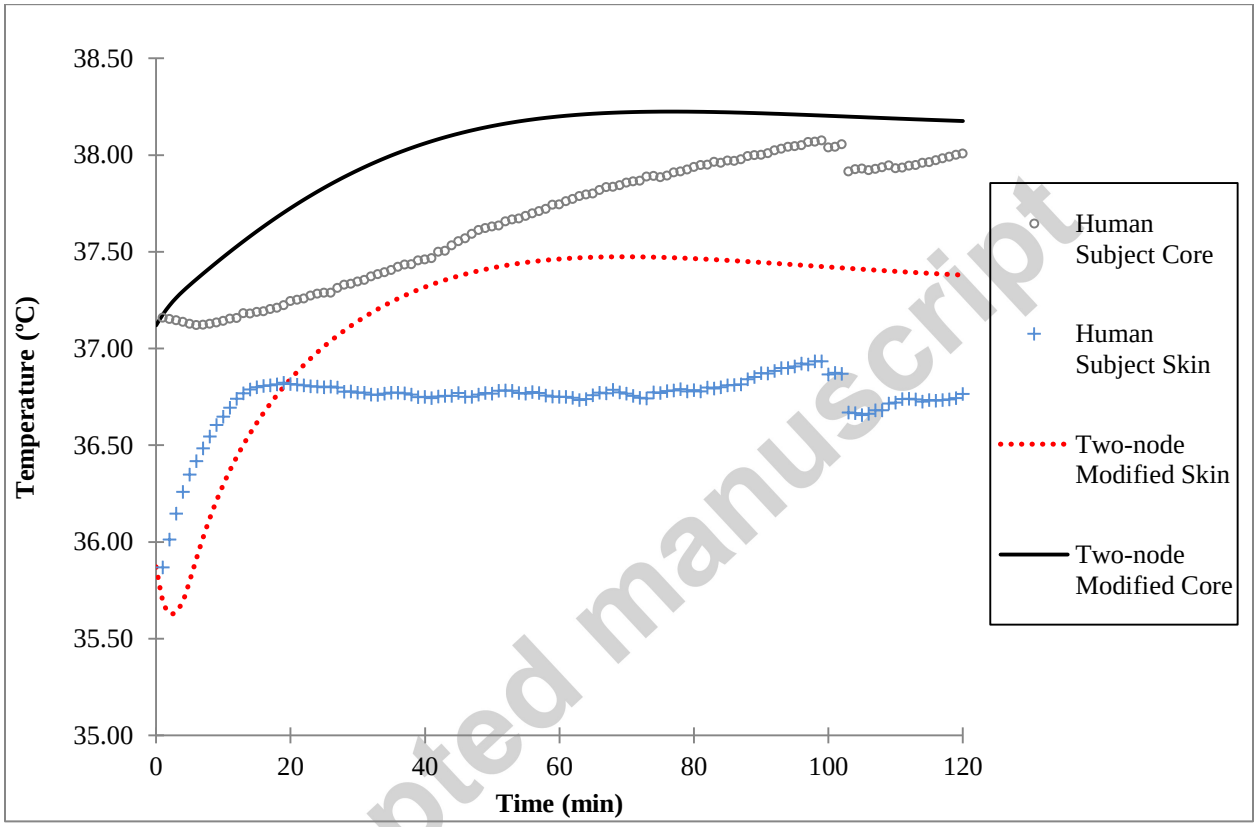

Figure 7 The results comparing the average of all the empirical data from the human subjects (HS) and the result of running the average subject through the modified two-node model (TNM).

In Figure 8, the skin wettedness factor for the original model is shown in two different data sets: potential skin wettedness, and actual skin wettedness. The potential skin wettedness is the value that was available for skin saturation, but was limited to unity, which is the actual skin wettedness in the non-wetting clothing assumption. The potential modified skin wettedness is shown to be over unity and the actual skin wetness for this value would be unity. However, the creation of the saturated area complicates this measure. For reference, the saturated area value, w_c is given as percentage of the body covered by the spot on the right axis of Figure 8.

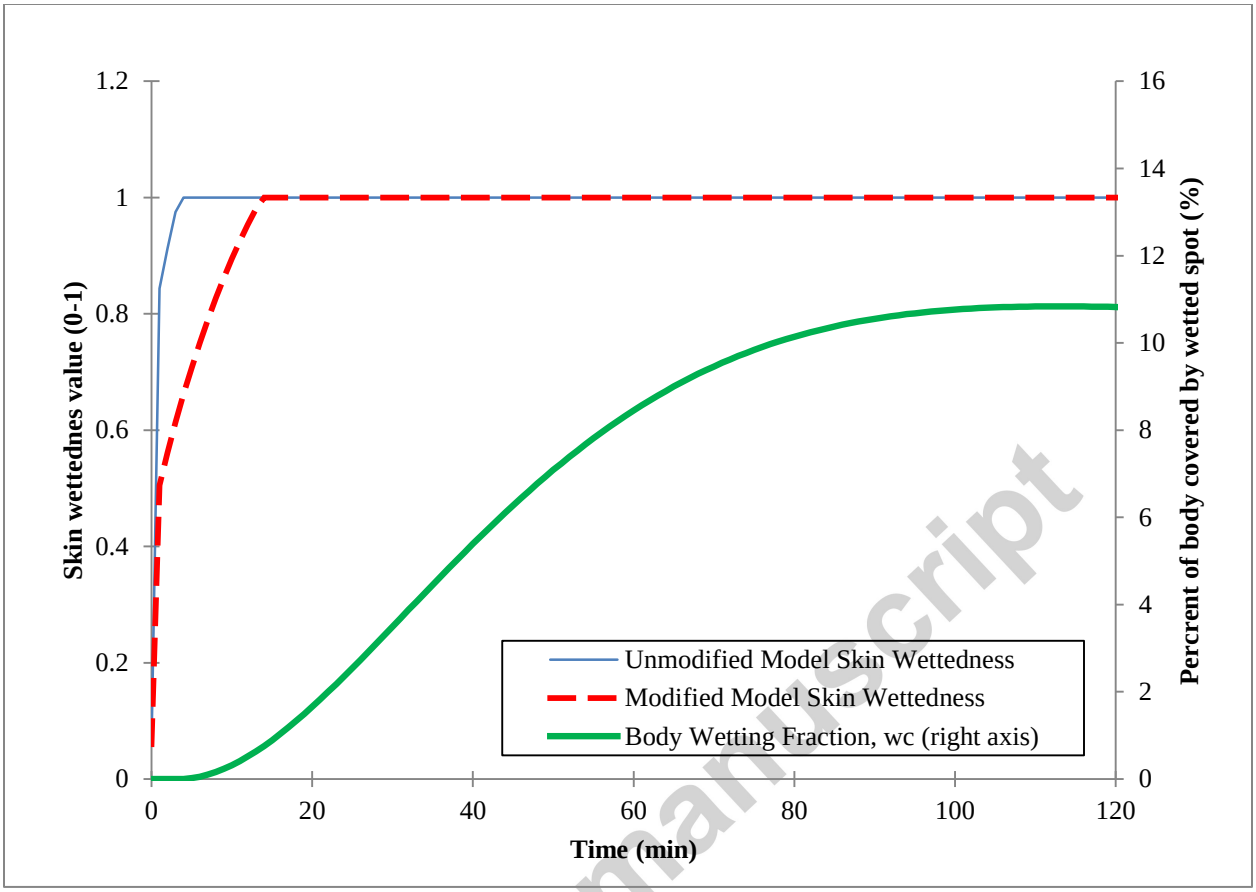

Figure 8 Skin wettedness on left axis for unmodified and modified two-node model. Percent of body surface covered by wetted spot in the modified two-node model is on the right axis.

The most disconcerting issue as shown in Figure 7 is the difference in inflection between the modified two-node model and the human subject graphs of core and skin temperatures. The human subject results indicate that the core and skin temperatures grew gradually throughout the test while in the simulations the core and skin temperatures grew quickly at the beginning of the test and then plateaued. Error analysis between the modeled average subject and the average value of all the subjects as shown in Figure 6 and Figure 7 for both the unmodified and modified two node models using Root Mean Square Error (RMSE) and Mean Absolute Error (MAE) are shown for the core and skin in Table 3.

Table 3 - Error calculations for the skin and core temperature of the average subject calculated with the two-node and modified two-node model compared with the average of the empirical data from 21 subjects using Root Mean Square Error (RMSE) and Mean Square Error (MSE).

	Root Mean Square Error	Mean Absolute Error
Two-Node Skin Temperature (°C)	1.91	1.83
Modified Two-Node Skin Temperature (°C)	1.30	1.29
Difference: Two-Node – Two Node Modified Skin Temperature(°C)	0.61	0.54
Two-Node Core Temperature (°C)	1.31	1.09
Modified Two-Node Core Temperature (°C)	0.55	0.47
Difference: Two-Node – Two Node	0.76	0.62

Modified Skin Temperature (°C)

Table 3 demonstrates that the average error values for the skin and core are very high, however the modified two-node model improves the RMSE for the core temperature by 0.76 to 0.55 and the MAE by 0.62 to 0.47. The skin temperature error is still high at an RMSE or 1.30 and MAE of 1.29. It is interesting that both the RMSE and MAE values are close to the standard deviations for the measured core temperature reported in Table 1 and Table 2. As a result of the magnitudes of both the standard deviations and the error values, error bars were omitted from Figure 6, Figure 7, and Figure 8 in order to produce clean and readable figures.

3.0 Discussion

The comparison of the two models to the human subject data above shows that the saturation of clothing, especially during work in uncompensable environments, can provide a significant amount of cooling to the body. This is not surprising, considering that this has been wondered about by scientists and engineers at least as far back as Fourt and Harris (1950). The proposed new model, as a modification to the existing human thermal models, improves prediction of the human subject results for soldiers exercising in uncompensable conditions compared to the ASHRE two-node model. The new boundary conditions account for the total sweat produced by the human subjects and incorporates a method to handle the sweat-saturating clothing in encapsulating, wetting garments.

Although the total sweat produced is accounted for in the mass balance, it is likely that a more accurate sweat model is needed. As was covered in the previous section, the paths of the core and skin temperatures in the simulation do not follow the same track to their similar ending temperatures. It is theorized that one main cause may be that the subjects sweat profusely at the beginning of the test; possibly during the setup time in the chamber; in preparation of exercise, or even because of the onset of exercise, and this is not captured in the model. Another possible reason for the difference in paths between the skin and core temperatures could be due to setting the skin and core temperatures to the values measured on the human subjects. It is possible that controlling for one of the values and letting the program determine the other at the start may be a better method for different applications. Similarly, the temperature set points associated with the sweat response may not be correct for this application or may have reacted poorly to the forced initialization. All of these values could conceivably act to reduce the error values reported at the end of the previous section.

This model uses fundamental principles to estimate the clothing properties for the saturated clothing. However, this method would be much improved through further research on the effects of saturated clothing on the thermal resistance of the clothing and air layer, which were estimated in this case based on literature. Also important to consider could be the effect of the saturated clothing, which was much colder than the surrounding clothing, likely coming into contact with the wearer as the person moved. This introduces a possible conduction heat transfer mechanism explored prominently in the work of Kerslake (1972), Havenith et al. (2008), and Wang et al. (2014). It is likely that the previously-studied efficiencies of the one-layer, tightly-fitting garments also contribute to the moisture-related heat transfer, especially where the garment is forced to come into contact with the skin by clothing, equipment, fitment, or drape. Therefore, it may be helpful when more data has been gathered on the subject of local fabric saturation percentages in real world us, to create separate areas expanding on the principles presented here regarding mass conservation and employing these efficiencies for tightly-fitting clothing found in the literature.

A large strength of this model is that it can be applied to more complicated multi-segment and multi-node models because it builds on fundamental principles. There are many multi-segment models such as Fiala's family of models (Fiala et al., 2012) which could use this methodology. In the case of models that incorporate local sweat rates and local clothing properties, this methodology can be applied to separate that segment into a non-wetting assumption and a saturated area. This method has the potential to improve their prediction capabilities in cases where encapsulating, wetting clothing is applied over the segment, especially incorporating new technology determining contact points between the body's surface and the clothing where moisture would be absorbed (Psikuta et al., 2012).

4.0 Conclusions

This work has quantified, using fundamental principles, the effects of saturated clothing on humans. This includes hot environments, especially those where encapsulating, wetting, and permeable clothing is worn. This new modified model mitigates part of the non-wetting clothing assumption that was presented and validated by conserving the overall sweat of the subjects. The presented work highlights the significant issues of using models with a non-wetting clothing assumption in uncompensable environments where clothing is likely to be soaked. However, more research is needed on the sweat rate of the subjects, clothing properties, and the speed at which clothing saturation takes place. The saturated-spot method is easily scalable to many different human thermal models employing non-wetting clothing assumptions. Despite the uncertainties, fixing the incorrect assumption for this case provided an excellent prediction of the final core temperatures of the human subjects in hot, uncompensable environments, considering the resolution of the model employed.

Acknowledgments: The human subject research used in the comparison of the models was generously funded by the United States Army as part of a separate project.

REFERENCES

ASHRAE, 2013. Fundamentals. ASHRAE, Atlanta, GA.
ASTM, 2010. Standard F2300-10, Standard Test Method for Measuring the Performance of Personal Cooling Systems Using Physiological Testing. ASTM International, West Conshohoken, PA, USA.
ASTM, 2016a. Standard F1291-16, Standard Test Method for Measuring the Thermal Insulation of Clothing Using a Heated Manikin. ASTM International, West Conshohoken, PA, USA.
ASTM, 2016b. Standard F2370-16, Standard Test Method for Measuring the Evaporative Resistance of Clothing Using a Sweating Manikin. ASTM International, West Conshohoken, PA, USA.
Danielsson, U., 1993. Convection coefficients in clothing air layers, Department of Energy Technology Division of Heating and Ventilation. The Royal Institute of Technology, Stockholm.
Elson, J., Eckels, S., 2015. An objective method for screening and selecting personal cooling systems based on cooling properties. Applied Ergonomics 48, 33-41.
Elson, J.C., McCullough, E.A., Eckels, S., 2013. Evaluation of personal cooling systems for military use, 15th International Conference on Environmental Ergonomics, Queenstown, New Zealand, pp. 281-284.
Fiala, D., Havenith, G., Bröde, P., Kampmann, B., Jendritzky, G., 2012. UTCI-Fiala multi-node model of human heat transfer and temperature regulation. Int J Biometeorol 56, 429-441.
Fourt, L., Harris, M., 1950. Physical Properties of Clothing Fabrics, in: Newburgh, L.H. (Ed.), Physiology of Heat Regulation and the Science of Clothing. Hafner Publishing Company, New York, pp. 291-319.
Gagge, A.P., Fobelets, A.P., Berglund, L.G., 1986. A standard predictive index of human response to the thermal environment.
Gagge, A.P., Nishi, Y., 1977. Heat exchange between human skin surface and thermal environment: biophysics and biophysiology, in: Falk, H.L., Murphy, S.D. (Eds.), Reactions to Environmental Agents.

Gagge, A.P., Stolwijk, J.A.J., Hardy, J.D., 1967. Comfort and thermal sensations and associated physiological responses at various ambient temperatures. Environmental Research 1, 1-20.
Hardy, J.D., 1950. Heat Transfer, in: Newburgh, L.H. (Ed.), Physiology of Heat Regulation and the Science of Clothing. Hafner Publishing Company, New York, pp. 78-108.
Havenith, G., Richards, M.G., Wang, X., Bröde, P., Candas, V., den Hartog, E., Holmér, I., Kuklane, K., Meinander, H., Nocker, W., 2008. Apparent latent heat of evaporation from clothing: attenuation and "heat pipe" effects. Journal of Applied Physiology 104, 142-149.
Jones, B.W., Ogawa, Y., 1992. Transient interaction between the human body and the thermal environment. ASHRAE Transactions 98, 189-195.
Jones, B.W., Ogawa, Y., 1993. Transient response of the human-clothing system. Journal of Thermal Biology 18, 413-416.
Katić, K., Li, R., Zeiler, W., 2016. Thermophysiological models and their applications: A review. Building and Environment 106, 286-300.
Kerslake, D.M., 1972. The stress of hot environments. Cambridge University Press.
Lotens, W.A., 1993. Heat transfer from humans wearing clothing. TU Delft, Delft University of Technology, Netherlands.
Pandolf, K.B., Givoni, B., Goldman, R.F., 1977. Predicting energy expenditure with loads while standing or walking very slowly. Journal of Applied Physiology 43, 577-581.
Psikuta, A., Frackiewicz-Kaczmarek, J., Frydrych, I., Rossi, R., 2012. Quantitative evaluation of air gap thickness and contact area between body and garment. Textile Research Journal 82, 1405-1413.
Stolwijk, J.A.J., 1971. A Mathematical Model of Physiological Temperature Regulation in Man. Yale University School of Medicine, Washington, D.C.
Stolwijk, J.A.J., Hardy, J.D., 1966. Temperature regulation in man — A theoretical study. Pflügers Archiv 291, 129-162.
Wang, F., Annaheim, S., Morrissey, M., Rossi, R., 2013. Evaporative cooling efficiency of one-layer tight fitting sportswear: a sweating torso manikin study, in: Cotter, J.D., Lucas, S.J., Mündel, T. (Eds.), 15th International Conference on Envionmental Ergonomics, Queenstown, NZ, pp. 285-287.
Wang, F., Annaheim, S., Morrissey, M., Rossi, R.M., 2014. Real evaporative cooling efficiency of one-layer tight-fitting sportswear in a hot environment. Scandinavian Journal of Medicine & Science in Sports 24, e129-e139.
Woodcock, A.H., 1962a. Moisture Transfer in Textile Systems, Part I. Textile Research Journal 32, 628-633.
Woodcock, A.H., 1962b. Moisture Transfer in Textile Systems, Part II. Textile Research Journal 32, 719-723.
Yi, L., Fengzhi, L., Yingxi, L., Zhongxuan, L., 2004. An integrated model for simulating interactive thermal processes in human–clothing system. Journal of Thermal Biology 29, 567-575.

Highlights:

- Presentation of a saturated clothing evaporation method.
- Discussion of models of moisture transport in clothing.
- Description of human subject testing in hot, desert environment.
- Demonstration of new method, uses, and assumptions.
- Comparison of new modeling method to existing method and human subject data.